DOI: https://doi.org/10.24425/amm.2026.1962

MARCIN GÓRNY[1*], BOGDAN CYGAN[2], JAN MAROSZ[1], GIULIANO ANGELLA[3]

ADVANCED DUCTILE IRONS FOR SPECIAL APPLICATIONS

Ductile iron is a highly versatile engineering material that offers an exceptional combination of strength, ductility, castability, and cost efficiency, making it a promising solution for a wide range of modern applications. This paper presents a concise review of advanced ductile iron grades, focusing on the relationships between microstructure and mechanical properties.

The analysis is based on a multiscale perspective, in which solidification processes, graphite quality, and matrix transformation are considered as intrinsically coupled phenomena governing material performance. Particular attention is given to the role of graphite morphology and distribution, as well as to the influence of solidification-induced heterogeneity on the formation of the metallic matrix.

It is shown that advanced ductile irons, including pearlitic ductile iron, ADI, IDI, Si-Mo, and Ni-Resist grades can be consistently interpreted within this framework, demonstrating their broad applicability and future potential as high-performance structural materials.

Keywords: Ductile iron; mechanical properties; impact strength; microstructure

1. Introduction

Ductile iron is one of the most widely used engineering materials, accounting for a significant share of global casting production (Fig. 1).

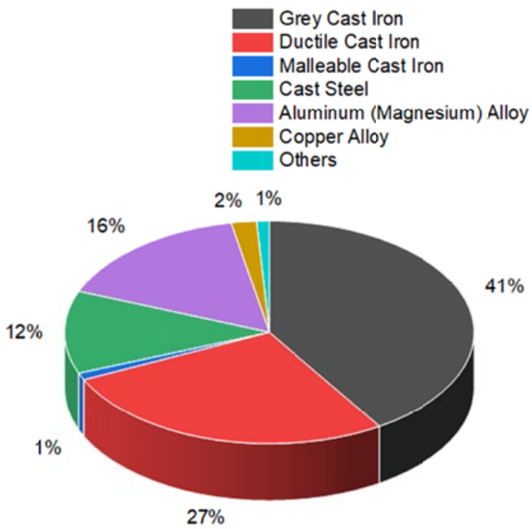

Fig. 1. Share of castings by materials type [1]

Its widespread application stems from a favorable combination of strength, ductility, castability, and cost efficiency, making it particularly attractive for automotive, energy, and heavy-duty engineering components. From a materials selection perspective, ductile iron offers a competitive balance between performance and cost, often outperforming alternative metallic materials when evaluated in terms of cost per unit yield strength (Fig. 2).

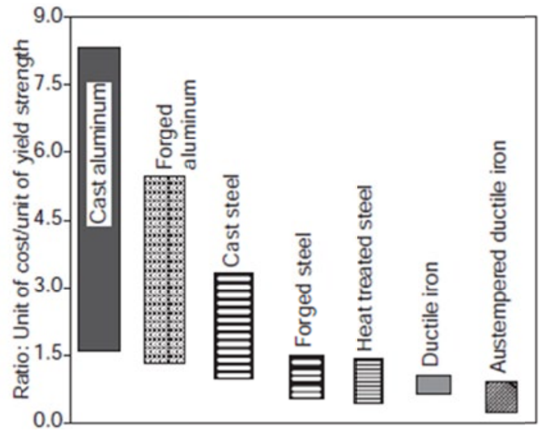

Fig. 2. Normalized index of relative cost per unit yield strength (forged steel = 1) for different metallic materials [2]

1 AGH UNIVERSITY OF KRAKOW, FACULTY OF FOUNDRY ENGINEERING, 23 REYMONTA STR., 30-059 KRAKOW, POLAND
2 TEKSID IRON POLAND, 49 CIĘŻAROWA STR., 43-430 SKOCZÓW
3 RESEARCH INSTITUTE CNR-ICMATE, UNIT OF MILANO, VIA R. COZZI 53, 20125 MILAN, ITALY

* Corresponding author: mgorny@agh.edu.pl

The microstructure of ductile iron consists of spheroidal graphite particles embedded in a metallic matrix, which may be in most cases ferritic, pearlitic, austenitic, or ausferritic depending on composition and processing route. While this description appears relatively simple, the relationships between microstructure and properties are governed by a complex interplay of solidification phenomena, graphite evolution, and phase transformations occurring over multiple length scales.

Despite extensive research, these aspects are often treated separately in the literature. Graphite morphology is typically analyzed in terms of nodularity and nodule count, solidification is described through dendritic growth models, and matrix formation is discussed within the framework of eutectoid or bainitic transformations. However, from a materials engineering perspective, these processes are intrinsically coupled, and their interaction ultimately determines the mechanical performance of ductile iron.

The aim of this work is to provide a comprehensive review of advanced ductile iron grades, including pearlitic, austempered (ADI), isothermally treated (IDI), Si–Mo, and austenitic (Ni-Resist) irons, with particular emphasis on the interrelationship between microstructure and properties. The selected grades represent advanced ductile iron families developed for special applications, including high-strength structural components, wear-resistant parts, cryogenic service, elevated-temperature operation, and corrosion-resistant engineering systems. A unified multiscale framework is proposed to interpret these relationships, highlighting the importance of integrating solidification, graphite characteristics, and matrix transformation in the design of high-performance ductile irons.

2. Microstructure-property relationships in ductile iron

2.1. Primary solidification and dendritic structure

Although ductile iron is typically designed as a near-eutectic or slightly hypereutectic alloy, solidification proceeds under non-equilibrium conditions that frequently lead to the formation of primary austenite dendrites [3-6]. The nucleation and growth of these dendrites are governed by local undercooling, thermal gradients, and microsegregation effects, which are particularly pronounced in thin-walled castings.

In hypereutectic compositions, primary graphite may nucleate prior to the eutectic reaction, whereas in near-eutectic alloys graphite formation is dominated by eutectic growth. Following the formation of primary austenite, solidification proceeds through the eutectic reaction, leading to the simultaneous growth of graphite nodules and austenite [3]. The interaction between eutectic growth and the pre-existing dendritic network plays a key role in determining the final microstructure.

The dendritic structure defines the spatial distribution of solute elements and second-phase particles. During solidification, graphite nodules interact with the advancing solid–liquid interface and may be either engulfed or pushed into interdendritic regions, depending on growth kinetics, interfacial energy balance, and local solidification rate [7-12]. As a result, graphite particles are often located in solute-enriched interdendritic zones, contributing to microstructural heterogeneity.

The interaction between the solidification front and particles of a foreign phase is schematically illustrated in Fig. 3, which shows both engulfment and pushing mechanisms and their

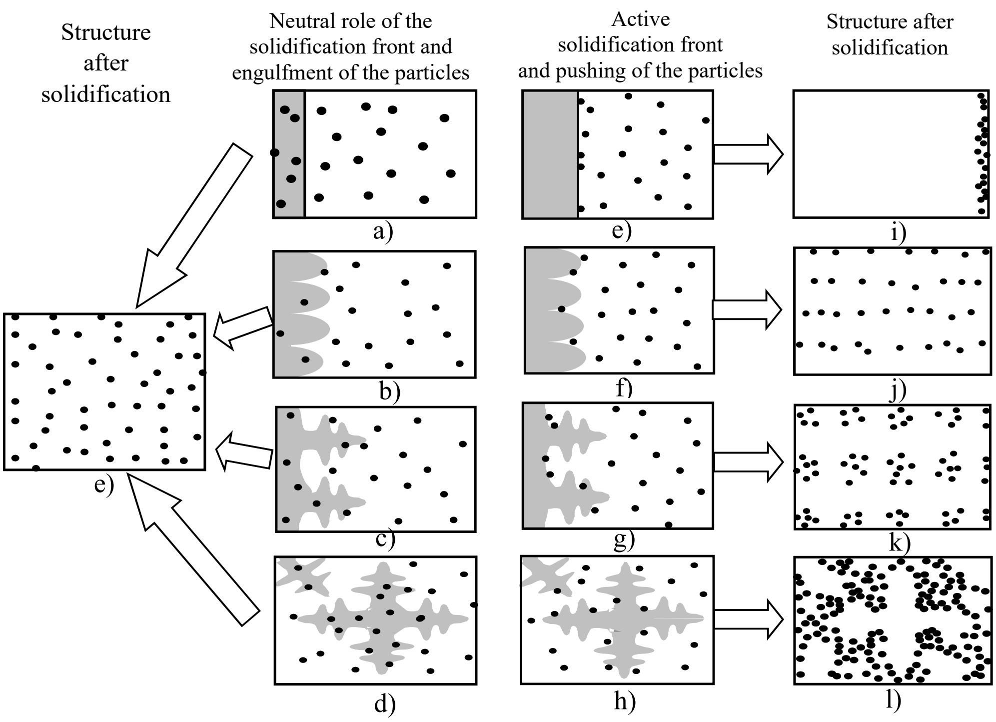

Fig. 3. Active and neutral role of the solidification front during its interaction with particles of an alien phase and the resulting microstructural effects; the solidification front during directional crystallization: a) flat, b) cellular, c) cellular-dendritic, d) solidification in volume, e), i)-l) final structure [13]

influence on the final structure [13]. The growth dynamics are additionally affected by the difference in thermal conductivity between graphite and the surrounding metallic matrix, which modifies local heat extraction conditions and influences the stability of the solidification front [7].

This heterogeneity directly influences subsequent solid-state transformations, as local variations in composition and cooling rate affect the formation of ferrite, pearlite, or more complex microstructures. Consequently, primary solidification establishes the initial spatial and compositional framework of the microstructure, which governs graphite distribution and strongly affects the evolution of the metallic matrix and, ultimately, the mechanical properties of ductile iron.

2.2. Graphite quality

Graphite quality is one of the most critical microstructural factors governing the mechanical behavior of ductile iron. From a materials engineering perspective, it should be understood as a combined effect of four key parameters: graphite fraction, nodule count, particle morphology, and spatial distribution. These parameters are interrelated and collectively determine the response of the material under mechanical loading [14].

The graphite fraction is predominantly dependent on carbon content and solidification path. In ductile irons, it typically ranges from approximately 2.8 to 3.8 wt.% C, corresponding to about 7-15 vol.%. For optimal properties, the composition should be close to eutectic, while slightly hypereutectic compositions are often preferred in thin-walled castings due to the high cooling rate, which influences the coupled eutectic zone [3]. However, despite nominally hypereutectic compositions, austenite dendrites are frequently observed under industrial conditions due to non-equilibrium solidification effects [4-6]. As a consequence, graphite nodules are often distributed inhomogeneously, typically within interdendritic regions or forming local clusters.

Nodule count is widely recognized as one of the most important indicators of melt quality and solidification conditions [6]. It reflects the nucleation potential of the liquid metal and integrates the effects of melt treatment, inoculation practice, and cooling rate. Increasing nodule count generally leads to a reduction in chilling tendency [15], modification of shrinkage behavior through pre-eutectic expansion, and a reduction in microsegregation intensity [16]. At the same time, higher nodule density decreases the average diffusion distance for carbon during the eutectoid transformation, promoting ferrite formation and contributing to a more homogeneous matrix. Typical values range from approximately 20 nodules/mm^2 in thick sections to a few thousand nodules/mm² in thin-walled castings [4,17]. It should be emphasized, however, that the beneficial effect of high nodule count is conditional upon a uniform spatial distribution [13].

Graphite morphology is another key parameter and is commonly evaluated using standardized image analysis methods, such as those defined in ISO 945 [18]. A widely used quantitative descriptor of graphite shape is the roundness parameter, defined as Eq. (1):

$$R = \frac{4\pi A}{l_m^2} \tag{1}$$

where A is the area of the graphite particle and l_m is its maximum Feret diameter. Based on this parameter, graphite particles are classified according to their deviation from an ideal spheroidal shape.

The overall nodularity N of ductile iron can then be expressed as Eq. (2):

$$N = \frac{\sum A_{(0.8\text{-}1.0)} + 0.5\sum A_{(0.6\text{-}0.8)}}{\sum A_{total}} \tag{2}$$

where $\sum A_{(0.8\text{-}1.0)}$ is the total area of graphite particles with high roundness (fully nodular), $\sum A_{(0.6\text{-}0.8)}$ corresponds to intermediate graphite shapes, and $\sum A_{total}$ is the total graphite area. It should be noted that different standards define nodularity using slightly different criteria, which may lead to variations in reported values [19].

The size distribution of graphite particles represents a fundamental statistical characteristic of ductile iron microstructure [20]. Numerous studies have demonstrated its strong influence on mechanical properties [20-21]. In thin-walled castings, a relatively narrow, unimodal size distribution is typically observed due to high cooling rates. In contrast, as section thickness increases and cooling rate decreases, the distribution often evolves toward bimodal or even trimodal forms, reflecting the coexistence of primary graphite, eutectic graphite, and secondary nucleation events. From the perspective of structural homogeneity, broad or multimodal distributions are generally less favorable.

The spatial distribution of graphite nodules remains one of the least quantitatively described aspects of graphite quality. Existing standards, such as ISO 945 [22], provide mainly qualitative classifications rather than absolute measures. Nevertheless, it is well established that non-uniform distributions particularly clustering in interdendritic regions may lead to local heterogeneity in mechanical response and promote crack initiation under load.

In summary, graphite quality should be regarded as a multidimensional parameter integrating composition, melt treatment, and solidification conditions. Its influence extends beyond individual characteristics, as the interaction between graphite fraction, morphology, and spatial distribution ultimately determines the effectiveness of load transfer and the overall mechanical performance of ductile iron.

2.3. Metallic matrixc formation

In addition to graphite morphology, the metallic matrix plays a decisive role in determining the final mechanical and functional properties of ductile iron. Depending on chemical composition, cooling rate, and post-solidification heat treatment, the matrix may consist of ferrite, pearlite, austenite, or more complex structures such as ausferrite, bainite or martensite. The matrix is formed during the eutectoid transformation of austenite and is strongly influenced by both solidification conditions and the spatial distribution of graphite nodules.

A key aspect, often overlooked in simplified descriptions, is the role of the primary structure, particularly the formation and evolution of austenite dendrites during solidification. Although ductile iron is typically designed as a near-eutectic or slightly hypereutectic alloy, numerous studies have shown that austenite dendrites may form even under nominally hypereutectic conditions, especially at high cooling rates characteristic of thin-walled castings [23-24]. This phenomenon is associated with local thermal and compositional fluctuations, as well as microsegregation effects during solidification.

The primary austenite phase may nucleate either at the mould wall or within the bulk liquid and grows in the form of dendritic structures, exhibiting columnar or equiaxed morphology depending on the temperature gradient and degree of undercooling. The resulting dendritic network plays a fundamental role in defining interdendritic regions, where solute enrichment occurs and where graphite nodules are frequently redistributed due to dendrite growth dynamics.

The interaction between dendrites and graphite nodules leads to the development of microstructural heterogeneity, which is particularly pronounced in thin-walled castings due to high cooling rates and short solidification times. Increasing cooling rate results in refinement of both the dendritic structure and graphite morphology, leading to a higher nodule count but also enhanced microsegregation of alloying elements. This microsegregation significantly affects the subsequent eutectoid transformation, thereby controlling the formation of ferrite and pearlite or, in the case of heat-treated alloys, ausferrite, bainite or martensite.

From a thermodynamic and kinetic perspective, the final matrix structure is governed by carbon diffusion distances (linked to nodule spacing), local chemical gradients resulting from dendritic solidification, the cooling rate through the eutectoid temperature range, and the presence of alloying elements such as Si, Ni, Mn or Mo.

In particular, a higher nodule count reduces the diffusion distance of carbon, promoting ferrite formation, whereas lower nodule density combined with stronger segregation tends to favor pearlite formation. These relationships become more complex in alloyed systems such as Si-Mo or Ni-Resist ductile irons, where matrix stability at elevated or cryogenic temperatures is of primary importance.

In the case of advanced ductile iron grades, such as austempered ductile iron (ADI), the initial as-cast microstructure including dendrite morphology and segregation pattern directly determines the effectiveness of subsequent heat treatment. Structural homogeneity of the austenite prior to austempering is essential for obtaining a uniform ausferritic matrix and high thermal stability.

Therefore, the metallic matrix should be regarded as the result of coupled processes occurring during both solidification and solid-state transformation. Its final morphology and phase composition are strongly dependent on the interplay between graphite distribution, dendritic structure, and chemical composition, which together determine the mechanical performance of ductile iron.

2.4. Multiscale interaction and property control

The above considerations demonstrate that the microstructure of ductile iron should be interpreted as a multiscale system in which primary solidification, graphite evolution, and matrix transformation are strongly coupled. Changes at one structural level inevitably influence the others, making isolated optimization of individual parameters insufficient for achieving desired properties.

This multilevel interaction can be used as a unified framework for interpreting the relationships between dendritic solidification, graphite quality, and matrix formation in relation to mechanical properties. The concept builds upon the mechanisms described above, integrating the effects of solidification dynamics [3], particle–interface interaction [7–13], and microstructure–property relationships [14]. Such an integrated perspective provides a consistent basis for understanding and comparing the behavior of advanced ductile iron grades discussed in the following sections.

3. Advanced ductile iron grades

3.1. Pearlitic ductile iron

High-strength ductile iron in the as-cast condition has undergone significant development in recent years, driven by the need to bridge the gap between conventional ferritic-pearlitic grades and heat-treated ADI, while maintaining cost and process simplicity. The achievable mechanical properties are governed, as mentioned previously, primarily by the solidification path, cooling rate, graphite quality, austenite dendritic network and solid state transformation (eutectoid transition).

A key factor controlling strength is the cooling rate, which directly influences both graphite quality and matrix refinement. In thin-walled castings, cooling rates can vary from 15 to 80°C/s, depending on section thickness and mould material, leading to a substantial increase in nodule count and refinement of pearlite, which in turn enhances strength (Fig. 4).

Higher nodule density reduces inter-nodular spacing and modifies carbon diffusion during the eutectoid transformation, promoting finer and more homogeneous microstructures. However, excessive cooling may increase the risk of carbides and structural inhomogeneity, requiring strict control of inoculation and melt quality.

Conventional as-cast ductile iron grades (EN-GJS-500–700) achieve tensile strengths up to 700 MPa through ferritic-pearlitic metallic matrix. Further strengthening can be obtained via solid solution strengthening (mainly by an addition of Si) and

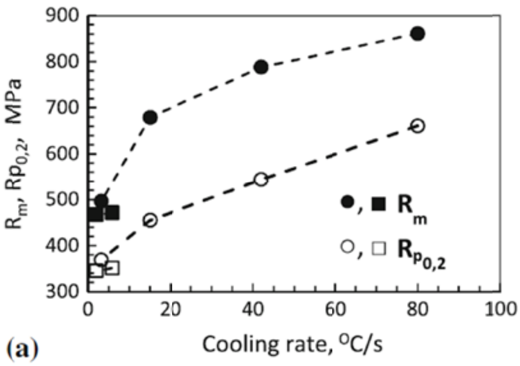

Fig. 4. Tensile and yield strength (a) as a function of cooling rate d, s-experimental points for SMS (furan-bonded silica sand) mold, j, h-experimental points for LDASC mold (furan-bonded Low-Density Alumina-Silicate Ceramic spheres) [24]

controlled pearlite stabilization (mainly through Cu, Mn, Sn). A representative example of advanced ductile iron is the SiboDur concept, in which moderate solid-solution strengthening by silicon is combined with controlled pearlite formation (typically via copper additions) [25-26]. An example of a casting made of SiboDur 700 ductile iron is shown in Fig. 5 together with its microstructure.

This approach enables a favorable balance between strength and ductility, while also improving energy absorption under dynamic loading compared to fully ferritic high-Si irons. Importantly, purely solid-solution-strengthened ferritic grades (e.g., EN-GJS-500-14) may exhibit limited resistance under impact conditions despite high elongation in static tests, highlighting the necessity of microstructural heterogeneity for dynamic performance [25].

Recent industrial developments demonstrate that the upper strength limit of as-cast ductile iron can approach or even exceed UTS ≈ 1000 MPa without austempering (Fig. 6). Data from Teksid Iron Poland indicate that pearlitic ductile iron with optimized chemistry (Ni, Cu) and process parameters can achieve UTS in the range of 950-1050 MPa, with yield strength above 600 MPa and elongation of ~5-9%. These properties are obtained through a combination of high nodularity (>90%), controlled graphite size, and a refined pearlitic matrix, often supported by relatively high nodule counts (e.g., 400-700 nodules/mm^2 depending on section thickness). Such materials are not yet fully

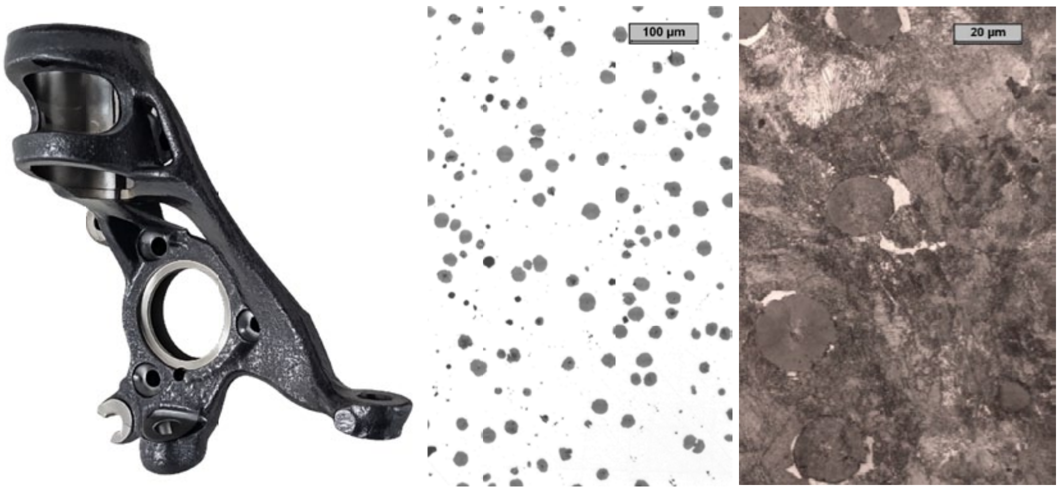

(a) (b) (c)

Fig. 5. Bionic lightweight design of steering knuckle made of SiboDur700 (a), graphite distribution (b) and microstructure after nital etching (c)

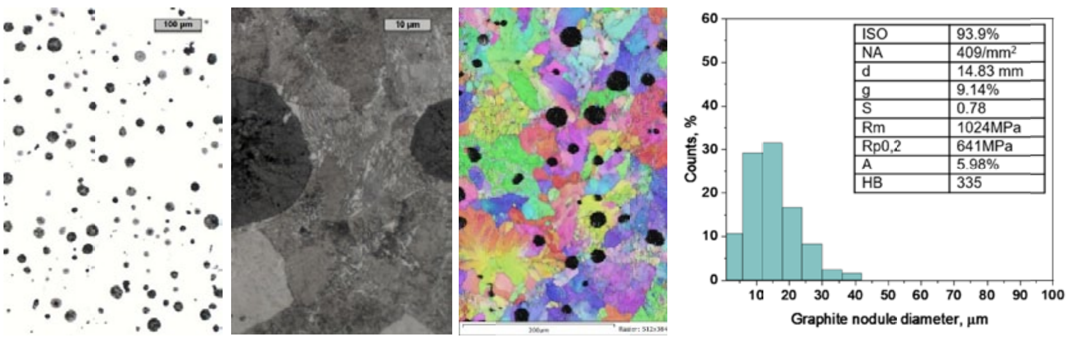

(a) (b) (c) (d)

Fig. 6. Microstructure of Advanced "Teksid" ductile iron (wall thickness 25 mm): a) graphite distribution, b) pearlitic metallic matrix, nital etched sample, c) EBSD image showing pearlitic colonies and d) histogram of graphite size distribution with microstructure parameters (ISO- nodularity, NA – number of graphite nodules, d – mean diameter of graphite nodules, g – graphite fraction, S – shape factor ($S = 4\pi A/P^2$, where A – surface area, P – perimeter)) and tensile properties

standardized but represent a competitive alternative to alloyed irons and even lower-grade ADI in selected applications.

From a metallurgical standpoint, the strengthening mechanisms in as-cast high-strength ductile iron are cumulative and include:

(i) pearlite fraction (>98%), both interlamellar spacing and pearlite colonies refinement,
(ii) solid solution strengthening (Si, Mn, Cu, Ni),
(iii) graphite nodules quality, ie. optimal combination of proper fraction, size and spatial distribution,
(iv) suppression of defects (porosity, degenerate graphite, inclusions, bi-film), which is particularly critical in thin sections.

Nevertheless, limitations remain. Increasing strength via pearlite and silicon typically reduces ductility (A = 5-9%) and impact toughness (charpy impact energy of Teksid-ductile iron amounts to about 50-60 J), and sensitivity to section thickness persists due to cooling-rate-dependent microstructure evolution.

In summary, state-of-the-art as-cast ductile iron can reach mechanical properties previously associated with heat-treated grades, provided that solidification conditions, chemistry, and inoculation (eutectic modification) are precisely controlled. Concepts such as SiboDur and the recent >1000 MPa class “Teksid” irons from industrial practice demonstrate that microstructural engineering at the casting stage alone can deliver high-performance materials, although often at the expense of reduced process robustness and narrower processing windows.

3.2. Austempered Ductile Iron (ADI)

Austempered ductile iron (ADI) represents one of the most advanced developments in cast iron metallurgy, offering a unique combination of high strength, ductility, wear resistance, and fatigue performance. Its properties are achieved through a controlled heat treatment process (Fig. 7).

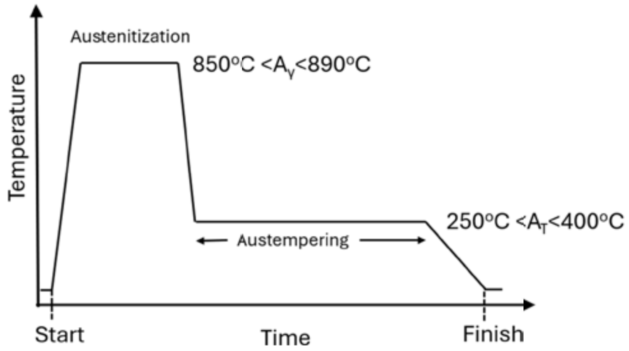

Fig. 7. Heat treatment scheme for ADI

The resulting microstructure, known as ausferrite, consists of acicular (bainitic) ferrite and carbon-enriched retained austenite, with occasional presence of martensite depending on the processing conditions (Fig. 8). The morphology and phase fractions are strongly governed by the austempering temperature and time. At lower temperatures, a high degree of undercooling promotes nucleation-dominated transformation, leading to a fine acicular ferrite structure and high strength. In contrast, higher austempering temperatures favour diffusion-controlled growth, resulting in coarser ferrite and increased retained austenite content, which enhances ductility and toughness.

The exceptional mechanical performance of ADI typically in the range of Rm = 1000-1700 MPa, $R_{p0,2}$ = 750-1500 MPa, elongation A = 3-20%, Charpy impact energy (unnotched samples) U = 80-230J, Vickers hardness ranges 280-600 HV [27]. The exceptional strength of ADI arises from a synergistic combination of strengthening mechanisms operating at multiple scales. The ferritic phase may exhibit a very high density of dislocations and dislocation loops, indicating significant strain hardening. Simultaneously, the austenite is strongly enriched in carbon (often approaching ~2 wt.%), leading to substantial solid-solution strengthening. Additionally, the austenite undergoes mi-

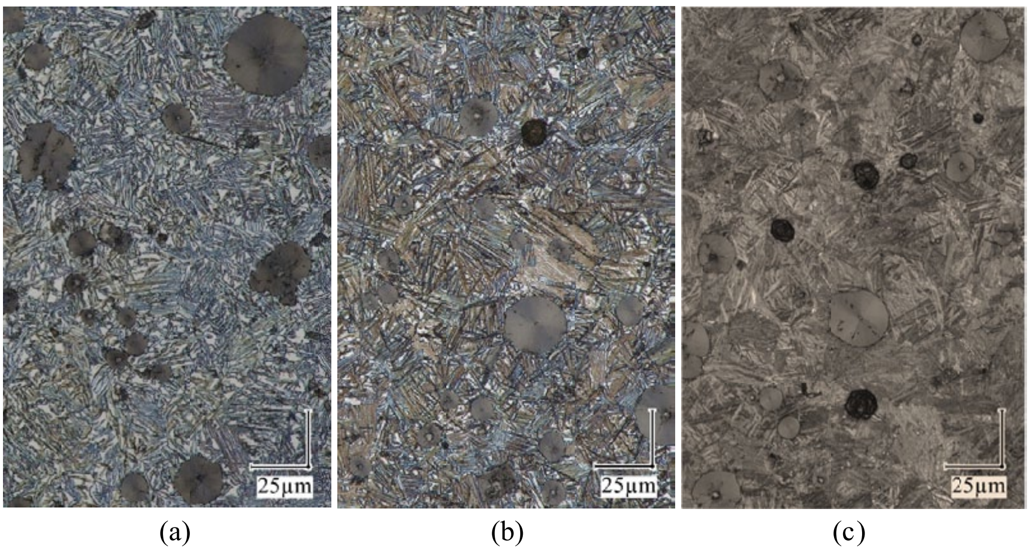

Fig. 8. Microstructure of austempered ductile iron (ADI) in 13 mm wall thickness castings, showing upper (a), intermediate (b), and lower (c) ausferrite. The heat treatment conditions comprised austenitisation at 875°C followed by austempering at 375°C (a), 300°C (b), and 250°C (c). Nital-etched samples

crostructural refinement through twinning and the formation of stacking faults, which introduce additional barriers to dislocation motion. These defects effectively subdivide grains and increase the density of coherent interfaces, further enhancing strength. The contribution of martensite, when present (especially in low-temperature austempered conditions), should also be considered, as its highly strained structure and dense network of microtwins significantly increase resistance to plastic deformation.

From a transformation perspective, the evolution of the ausferritic structure is governed by a competition between bainitic ferrite growth and carbon partitioning into austenite. The austempering temperature controls both the nucleation rate of ferrite and the diffusion kinetics of carbon. Lower austempering temperatures result in finer bainitic ferrite and limited carbon redistribution, while higher austempering temperatures promote carbon diffusion and stabilization of retained austenite, often leading to the formation of blocky austenite. A critical aspect of ADI is the stability of retained austenite, which directly influences mechanical performance. Carbon-enriched austenite can undergo stress-induced transformation into martensite (TRIP effect), providing additional work hardening and delaying strain localization. However, the effectiveness of this mechanism depends strongly on the morphology and stability of austenite. Film-like austenite, located between ferrite laths, exhibits higher stability and contributes positively to toughness, whereas coarse blocky austenite may transform prematurely or even during cooling, reducing ductility and impact resistance. The kinetics of the austempering process can be divided into two stages. In Stage I, carbon partitions from supersaturated ferrite into austenite, stabilizing it and leading to the formation of a carbide-free ausferritic structure. In Stage II, prolonged holding results in the decomposition of austenite into ferrite and carbides (e.g., Fe_3C), which significantly deteriorates toughness and should be avoided in practical applications.

From an application perspective, ADI offers a superior strength-to-weight ratio compared to steels, combined with good castability and vibration damping. This makes it particularly attractive for dynamically loaded components such as gears, crankshafts, suspension elements, and heavy-duty structural parts (Fig. 9).

However, the material is sensitive to processing parameters, section thickness, and initial microstructure, which require careful control to ensure reproducible performance.

ADI should be regarded as a highly engineered multiphase material system in which the final properties result from the interplay between solidification structure, graphite morphology, phase transformation kinetics, and microstructural stability. The balance between strength and ductility is primarily governed by the morphology and stability of retained austenite, as well as the scale and defect structure of bainitic ferrite, making precise control of the austempering process essential for achieving optimal performance. As reported in [29] the issue of thermal stability is of great practical importance, as it significantly affects the conditions in which cast components made of high-quality ADI cast iron can be used. The formation of a homogeneous microstructure without blocky austenite regions is strongly governed by the heat treatment parameters, in particular the austenitizing temperature which significantly affects the lattice parameters of austenite and ferrite, their fractions as well as the strain state within these phases in ADI. An increase in the austenitizing temperature, although leading to a higher carbon content in austenite prior to austempering, does not necessarily result in a higher carbon concentration in the retained austenite after austempering. It was observed [29] that ADI produced at a lower austenitizing temperature exhibits a higher austenite lattice parameter indicating a higher thermal stability compared to ADI obtained at a higher austenitizing temperature (Fig. 10).

a) b) c)

Fig. 9. Examples of ADI parts: a) Differential flange (ADI 800-10), b) Delimber blade (ADI 1200-3), c) Steering knuckle (ADI 900-8) [28]

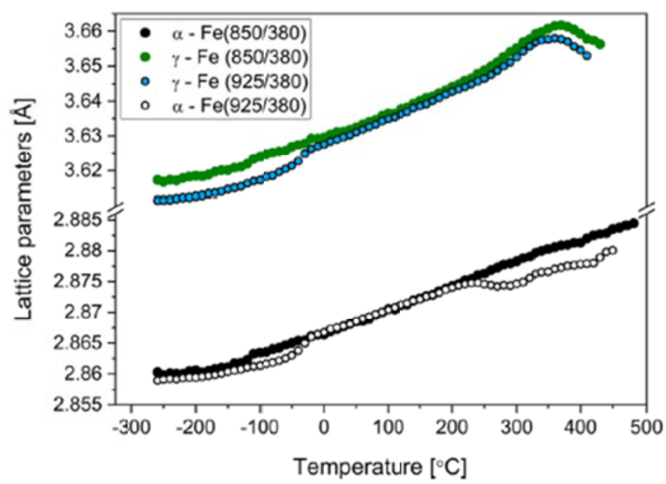

Fig. 10. Lattice parameters as a function of the temperatures of 850/380 and 925/380 ADI (wall thickness of 25mm) [29]

3.3. Isothermed Treated Ductile Iron (IDI)

Isothermed Ductile Iron (IDI) represents a recently developed class of ductile irons, introduced to address the economic and technological limitations of conventional ADI grades [30-31]. This material, developed by Zanardi Fonderie, is defined as a ferritic-pearlitic ductile iron obtained through isothermal heat treatment of ferritic base iron, without the use of alloying additions (Fig. 11).

From a technological standpoint, the IDI production route involves intercritical austenitization followed by rapid cooling in a salt bath, leading to the transformation of austenite into quench pearlite while retaining proeutectoid ferrite. In contrast to ADI, where an ausferritic microstructure is targeted, IDI develops a so-called perferritic structure, consisting of an interconnected network of ferrite and pearlite. The microstructure of IDI comprises proeutectoid ferrite and pearlite formed as a result of intersecting the "pearlitic nose" on the CCT diagram (Fig. 11a). The pearlite fraction typically ranges from 40 to 70%, while graphite is present in a spheroidal form. This phase arrangement differs significantly from the conventional ferrite-pearlite distribution in pearlitic ductile iron, resulting in a distinct deformation mechanism and an improved balance between strength and ductility.

IDI can be considered an intermediate material between pearlitic ductile iron and ADI. As demonstrated in studies by Zanardi, its mechanical properties are comparable in strength to pearlitic grades, while exhibiting significantly higher toughness and ductility due to the presence of ferrite and a more homogeneous microstructure. In particular, the tensile strength typically ranges from 800 to 950 MPa, with a yield strength of 450-580 MPa, elongation of 6-12%, impact energy (unnotched samples) 50 J to more than 90 J and hardness 220-290 HBW depending on section thickness and intercritical austenitization conditions.

A key advantage of IDI is the absence of alloying elements (especially Mo, Cu and Ni), which reduces costs and possible segregation and limits the sensitivity of properties to section thickness. It should be emphasized that a homogeneous metallic matrix composed of proeutectoid ferrite and pearlite can be achieved in castings across a wide range of section thicknesses, from thin-walled to over 60 mm, which is crucial for structural design. At the same time, this translates into lower production costs compared to ADI, while maintaining competitive performance.

In terms of fatigue behavior, IDI exhibits properties intermediate between pearlitic ductile iron and ADI. The fatigue limit in rotating bending is approximately 380 MPa, which is lower than that of typical ADI grades but significantly higher than that of conventional pearlitic irons. Similarly, impact resistance shows intermediate values, while the temperature-dependent behavior is comparable to lower-grade ADI.

An important practical aspect is the very good machinability of IDI. Due to its moderate hardness and structural uniformity, the material can be machined similarly to ferritic-pearlitic ductile iron of comparable hardness, while offering improved mechanical properties. This makes IDI particularly attractive for components requiring machining after casting.

In summary, IDI represents a promising material alternative that bridges the gap between pearlitic ductile iron and ADI. It combines moderately high strength, good ductility, enhanced structural uniformity, and lower production costs. Therefore, it can be effectively applied in components where the full performance potential of ADI is not required, while conventional pearlitic ductile irons fail to provide sufficient service properties.

3.4. Si–Mo Ductile Iron

Silicon–molybdenum ductile iron (Si–Mo DI) constitutes a distinct class of ferritic ductile irons designed primarily for high-temperature service, where thermal stability, oxidation resistance, and dimensional integrity are critical. According to the classification defined in European Standard EN 16124 [32], Si–Mo grades (e.g., EN-GJS-SiMo45-6) belong to heat-resistant ductile irons intended for operation at temperatures exceeding ~600-750°C, particularly in cyclic thermal conditions typical of exhaust systems and furnace components.

The microstructure of Si–Mo ductile iron in the as-cast condition is predominantly ferritic, containing spheroidal graphite and a minor fraction of pearlite and carbides (Fe_2MoC and M_6C) (Fig. 12).

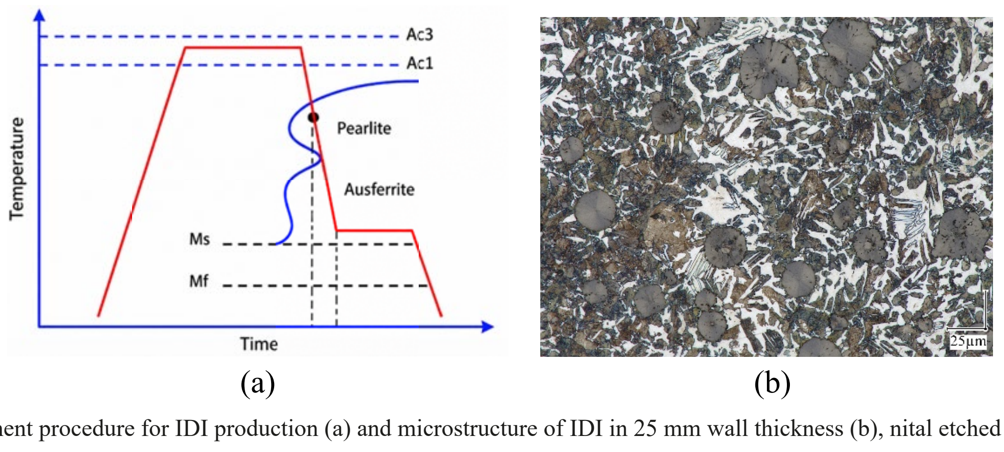

(a) (b)

Fig. 11. Heat treatment procedure for IDI production (a) and microstructure of IDI in 25 mm wall thickness (b), nital etched sample

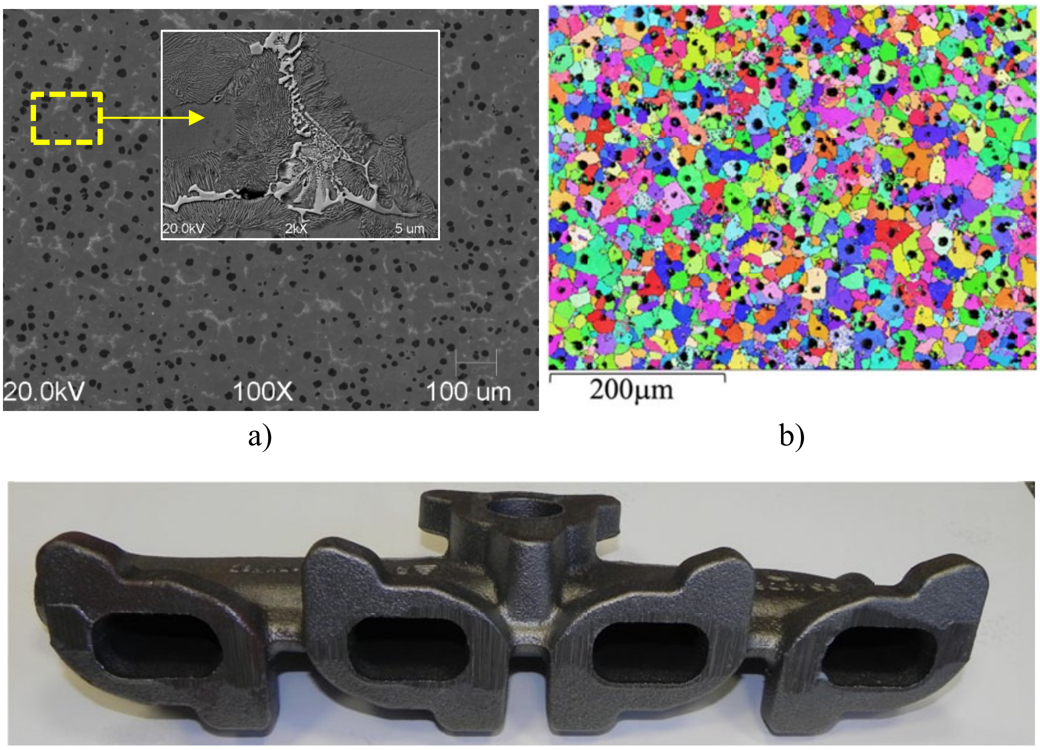

a) b)

c)

Fig. 12. SEM (a) and EBSD (b) microstructure of Si-Mo ductile iron [33], c) exhaust manifold made of Si-Mo ductile iron [34]

From a solidification perspective, Si–Mo ductile iron typically solidifies as a slightly hypereutectic alloy, with primary graphite precipitation followed by eutectic transformation. A key feature distinguishing this material from conventional ferritic ductile irons is the pronounced role of microsegregation, especially of Mo and C, which governs the formation of intercellular carbides and pearlite. Importantly, as demonstrated experimentally, the occurrence of these phases is not primarily controlled by cooling rate at the eutectoid transformation, but rather by segregation phenomena established during solidification [35]. Cooling rate remains, however, a critical parameter controlling the final microstructure at multiple scales. Increasing cooling rate (e.g., in thin-walled castings of 3-5 mm) leads to: refinement of graphite nodules (higher nodule count, smaller size), increased ferrite fraction, reduction of microsegregation intensity, and consequently suppression of carbide and pearlite formation. Conversely, lower cooling rates in thicker sections promote segregation-driven precipitation of carbides in intercellular regions, often forming a characteristic network morphology. This carbide skeleton, while detrimental to ductility, significantly enhances high-temperature strength, creep resistance, and dimensional stability properties that are essential for exhaust manifolds and turbine housings.

A particularly important aspect of Si-Mo ductile iron is its microstructural stability during long-term thermal exposure. The ferritic matrix, stabilized by high silicon content (typically 4-5 wt.%), exhibits low diffusion rates and resistance to phase transformation, while molybdenum improves creep resistance and limits coarsening of the microstructure. At the same time, the presence of stable carbides contributes to maintaining mechanical integrity under prolonged high-temperature loading.

However, this stability is intrinsically linked to the solidification path and resulting microsegregation. As evidenced by both experimental observations and Thermo-Calc simulations, the distribution of Mo and C during solidification determines the spatial localization of carbides and pearlite. This leads to a heterogeneous microstructure, particularly in thicker castings, where intercellular regions may become enriched in alloying elements. Such heterogeneity can be beneficial for high-temperature strength but may negatively affect room-temperature ductility and machinability. An additional feature of Si–Mo ductile iron is its relatively low sensitivity to cooling rate (Fig. 13) compared to unalloyed ductile irons when assessed through global properties such as ultrasonic wave velocity. This behaviour is attributed to the compensating effects of graphite morphology and carbide fraction: while higher cooling rates increase nodule count and ferrite content, slower cooling enhances carbide formation, which partially offsets changes in mechanical response.

From a microstructural design perspective, achieving optimal performance in Si–Mo ductile iron requires controlling not only the cooling rate but also the uniformity of graphite distribution and the extent of segregation. As reported in [34] ultra-thin-walled Si–Mo ductile iron castings can be produced by investment casting with wall thicknesses down to ~1 mm. The in-situ formation of (Ti,Mo)C carbides via the SHSB process results in a uniform dispersion of fine particles (~5 vol.%, <5 μm), which refine the microstructure and suppress the formation of eutectic M_6C carbides. As a result, the material exhibits improved

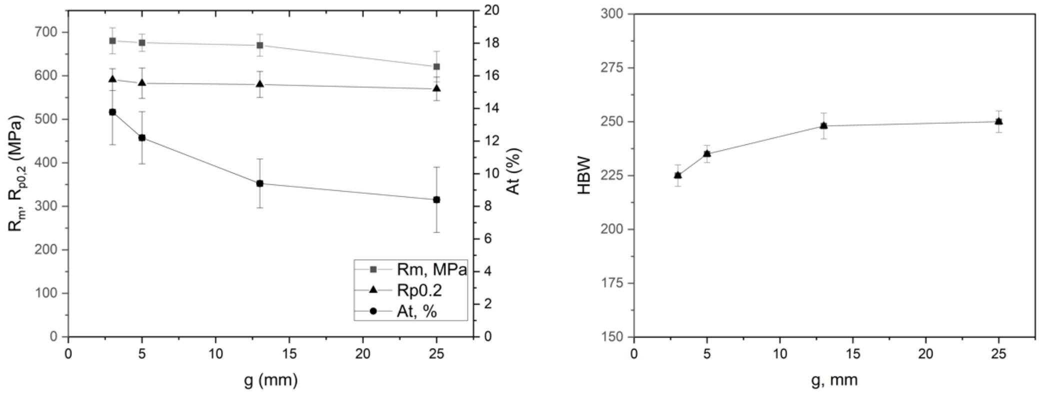

(a) (b)

Fig. 13. (a) Tensile, yield strength, and elongation; (b) hardness of Si-Mo ductile iron (N-GJS-SiMo45-6) as a function of casting wall thickness [36]

ducti_lity, toughness, and high-temperature stability, while maintaining excellent surface quality. This approach enables new possibilities for thin-walled, high-temperature components beyond the limitations of conventional Si–Mo alloys.

In summary, Si–Mo ductile iron should be considered a segregation-controlled, thermally stable ferritic system, in which the final properties result from the interplay between solidification conditions, graphite morphology, and the distribution of Mo-rich carbides. Its superior high-temperature performance arises not from a single strengthening mechanism, but from a complex balance between ferritic matrix stability, controlled carbide precipitation, and resistance to microstructural coarsening during service.

3.5. Austenitic (Ni-Resist) Ductile Iron

Austenitic ductile iron, commonly referred to as Ni-Resist ductile iron, constitutes a distinct class of cast irons with spheroidal graphite and a fully austenitic metallic matrix stabilized by a high nickel content, typically in the range of 18-36 wt.%. The material is standardized, among others, in ISO 2892 [37], where grades such as S-NiCr 20-2 or S-Ni 22 (e.g., EN-GJSA-XNi22) define both chemical composition and expected performance characteristics. The key role of nickel is to suppress the $\gamma \rightarrow \alpha$ transformation, thereby ensuring the stability of the austenitic phase over a wide temperature range, from cryogenic conditions (down to approximately −200°C) up to elevated temperatures approaching 1000-1050°C.

The microstructure of austenitic ductile iron is governed by solidification phenomena and consists of primary austenite dendrites followed by eutectic transformation, resulting in graphite nodules embedded within the austenitic matrix. Detailed studies [23] show that the dendritic structure is highly developed and branched, with graphite preferentially located in interdendritic regions and along austenite grain boundaries (Fig. 14).

This morphology reflects the solidification path and influences both microsegregation and defect formation, including porosity and graphite distribution heterogeneity. Furthermore, the weak segregation tendency of nickel (partition coefficient close to unity) leads to relatively uniform austenite chemistry compared to other alloying elements, which contributes to structural stability [38].

The presence of spheroidal graphite is essential for achieving a favourable combination of mechanical properties. Compared to flake graphite alloys, the nodular morphology

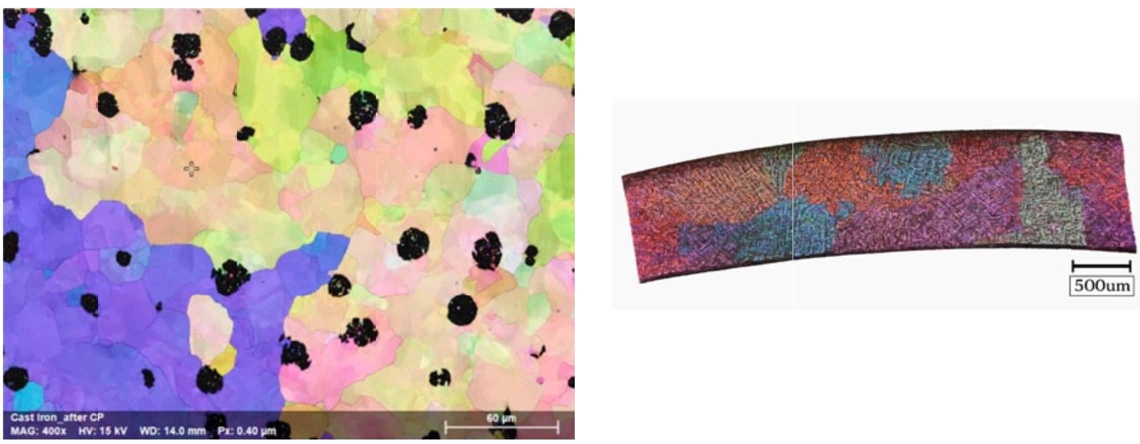

a) b)

Fig. 14. EBSD microstructure for high-nickel SGI [23] (a), ultra-thin-walled casting (wall thickness of 1mm) made of high-nickel ductile iron (D-5S)

significantly improves ductility and strength, which explains the increasing industrial importance of ductile Ni-Resist grades. Typical mechanical properties include tensile strength exceeding 500 MPa and elongation that may surpass 40%, impact properties as high as up to 200 J, depending on composition and the presence of carbide-forming elements. The austenitic matrix, due to its FCC crystal structure, provides a high number of slip systems, enabling excellent plastic deformation capability even at low temperatures.

A critical aspect of this material system is the strong dependence of properties on chemical composition, particularly the contents of nickel and chromium. Nickel is responsible for stabilizing austenite, improving corrosion resistance, and controlling thermal expansion. Increasing nickel content enhances structural stability and extends the operational temperature range, while also affecting magnetic properties by reducing ferromagnetic behaviour and enabling non-magnetic applications. Chromium, on the other hand, promotes the formation of carbides (e.g., M_7C_3), which increase hardness, wear resistance, and corrosion resistance, especially at elevated temperatures, but simultaneously reduce ductility and impact toughness due to the formation of brittle networks along grain boundaries.

From the recent work [38-39] it follows that the balance between nickel and chromium content enables the tailoring of properties depending on application requirements. Partial substitution of nickel with chromium may maintain corrosion resistance while reducing cost, but at the expense of plastic properties. Additionally, a minimum nickel content of approximately 25 wt.% is sufficient to ensure full austenitic stability even under cryogenic conditions, which is critical for applications in extreme environments.

Another key feature of austenitic ductile iron is its exceptional resistance to corrosion, erosion, and high-temperature oxidation [40-41]. Compared with conventional ferritic or pearlitic ductile irons, Ni-Resist alloys exhibit significantly improved behaviour in aggressive environments such as seawater, weak acids, and high-temperature gases. The oxide layers formed on the surface are adherent and protective, which contributes to long-term durability. At the same time, the absence of phase transformations in the austenitic matrix eliminates problems related to thermal expansion mismatch and transformation-induced stresses, which are typical for ferritic-pearlitic cast irons at elevated temperatures.

From a structural perspective, recent studies emphasize the importance of the interplay between dendritic solidification, graphite morphology, and matrix chemistry. Variations in wall thickness affect the number and size of graphite nodules, while maintaining relatively homogeneous mechanical properties across sections. This indicates that, despite microstructural heterogeneity at the mesoscale, the austenitic matrix provides robust property stability (Fig. 15).

In summary, austenitic ductile iron is a highly specialized material system in which the combination of spheroidal graphite and a fully austenitic matrix ensures excellent ductility, corrosion resistance, and thermal stability over an exceptionally wide temperature range. Its properties are primarily controlled by nickel-driven phase stability and modified by carbide-forming elements such as chromium. The recent works of Bork et al. clearly demonstrate that microstructural design particularly the control of dendritic structure, graphite distribution, and alloying balance enables precise tailoring of mechanical and functional properties, making this class of cast irons uniquely suited for demanding applications in automotive (Fig. 16), energy, chemical, and cryogenic engineering.

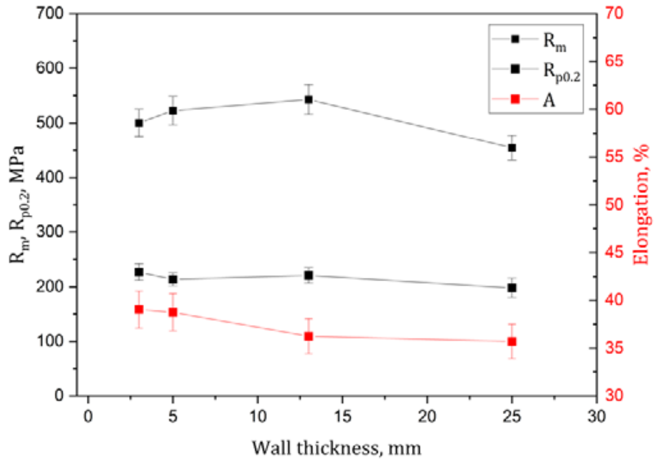

Fig. 15. Tensile properties for high-nickel (GJSA-XNi 22) ductile iron as a function of casting wall thickness [41]

Fig. 16. Turbine manifolds and housings for automotive gasoline powered engines. Ni-Resist D-5S [40]

4. Conclusions

The present review demonstrates that ductile iron should be interpreted not as a simple composite of graphite and metallic matrix, but as a multiscale material system, in which solidification, graphite evolution, and phase transformation are intrinsically coupled. The mechanical and functional properties of ductile iron are therefore governed by interactions occurring across multiple structural levels, from atomic-scale phenomena to macroscale heterogeneity.

At the primary level, dendritic solidification can play a decisive role even in eutectic or hypereutectic compositions. The formation of austenite dendrites controls solute redistribution and defines interdendritic regions, where graphite nodules are preferentially located. This interaction strongly affects graphite spatial distribution and contributes to microstructural inhomogeneity, particularly in thin-walled castings. At the eutectic level, graphite quality defined by its fraction, nodule count, morphology, and spatial distribution remains the key parameter controlling mechanical behaviour. In particular, high nodule density and a narrow size distribution reduce stress concentration effects and shorten diffusion distances during eutectoid transformation, thereby promoting more homogeneous and refined matrix structures. At the matrix level, the final properties are determined by the transformation of austenite into ferrite, pearlite, ausferrite, or austenite, depending on alloy composition and processing route. This transformation is strongly influenced by microsegregation inherited from solidification, highlighting the fundamental link between casting conditions and final performance. In advanced grades such as ADI, IDI, Si–Mo, and Ni-Resist ductile irons, additional mechanisms including austempering transformation, segregation-controlled carbide formation, and austenite stabilization further extend the achievable property range.

The multilevel interactions described above are schematically summarized in Fig. 17, which provides a unified framework linking primary solidification, graphite morphology, and matrix transformation with mechanical properties. This framework emphasizes that optimization of ductile iron cannot be achieved through isolated control of individual parameters, but requires an integrated approach combining alloy design, melt treatment, and solidification control.

From a practical perspective, recent developments indicate that advanced ductile irons including high-strength as-cast pearlitic grades can approach or even partially replace heat-treated materials in selected applications. At the same time, specialized alloys such as ADI, IDI, Si–Mo, and Ni-Resist provide tailored solutions for extreme service conditions, including high-temperature and cryogenic environments. Future research should therefore focus on integrated multiscale design strategies, supported by advanced characterization and modelling tools, to further improve the predictability and performance of ductile iron systems.

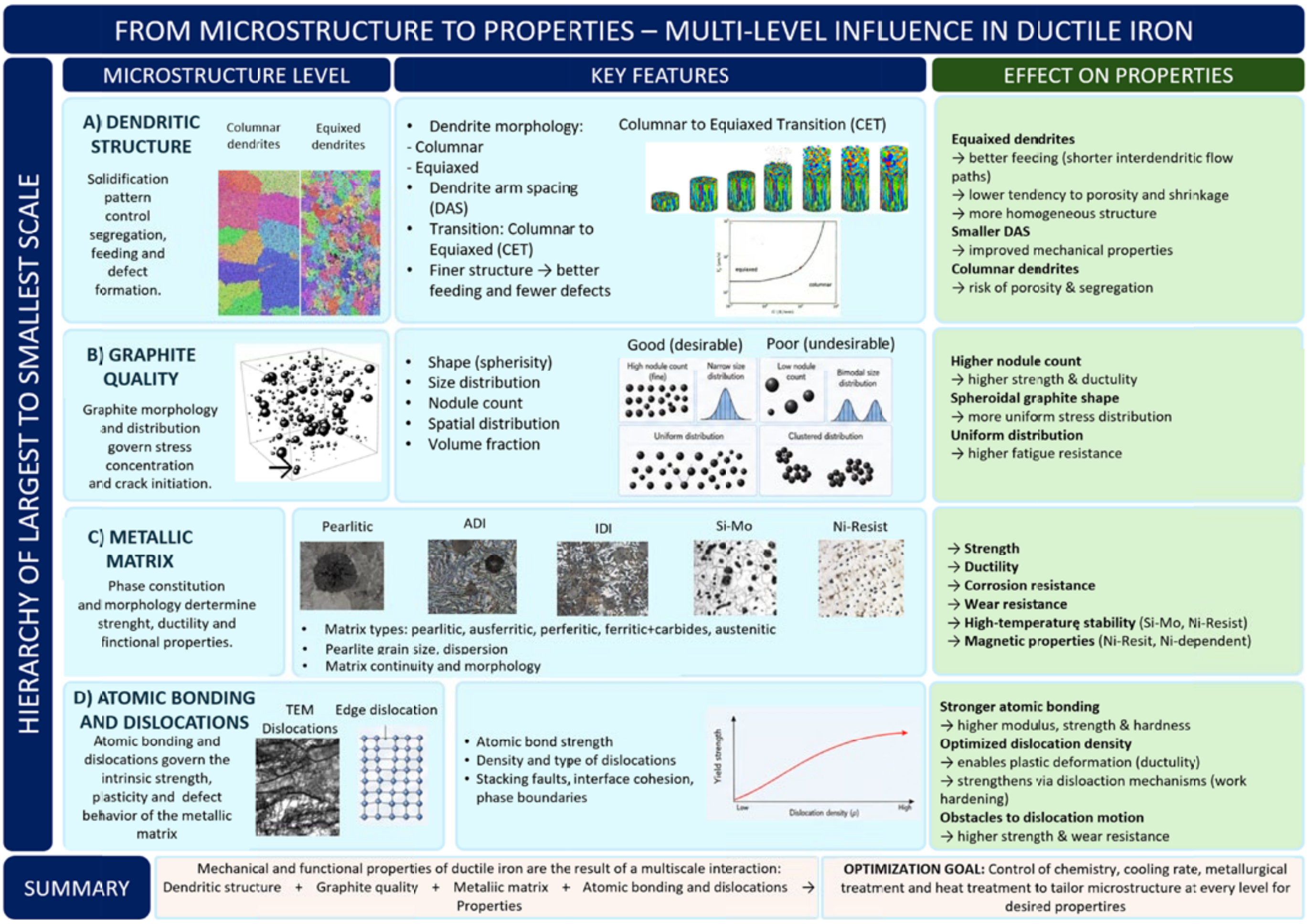

Fig. 17. Unified multiscale framework illustrating the relationships between solidification, graphite morphology, matrix transformation, and mechanical properties in conventional and advanced ductile iron grades (pearlitic, ADI, IDI, Si–Mo, Ni-Resist)

Dedication

The authors dedicate this work to Professor Paweł Zięba on the occasion of his 70th birthday, honoring his outstanding contributions to materials science and his lasting impact on the field of metallurgy.

Acknowledgments

This research was conducted within the Horizon Europe Project No. 101159771 – NetCastPL4.0.
This work was also carried out as part of research funded by a subsidy from the Ministry of Science and Higher Education and conducted at the Department of Engineering of Alloys and Composites, Faculty of Foundry Engineering, AGH University of Krakow.

REFERENCES

[1] World Foundry Organization, WFO Global Foundry Report 2025: Actual Situation of the Worldwide Casting Industry, World Foundry Organization Ltd., United Kingdom (2026).

[2] K.L. Hayrynen, ADI: Another Avenue for Ductile Iron Foundries, Mod. Cast. (Aug. 1995), 35-37.

[3] D.M. Stefanescu, Science and Engineering of Casting Solidification, 3rd ed., Springer, Cham (2015).

[4] M. Górny, D.M. Stefanescu, Thin-wall ductile iron castings. In: ASM Handbook **1A**, ASM Int. 626-628 (2017).

[5] R. Ruxanda, L. Beltran-Sanchez, J. Massone, D.M. Stefanescu, On the Eutectic Solidification of Spheroidal Graphite Iron – An Experimental and Mathematical Modeling Approach. AFS Trans. **109**, 1037-1048 (2001).

[6] E. Fraś, H.F. Lopez, Eutectic Cells and Nodule Count – An Index of Molten Iron Quality. Int. J. Metalcast. **4**, 35-61 (2010).

[7] D.M. Stefanescu, B.K. Dhindaw, S.A. Kacar, A. Moitra, Behavior of ceramic particles at the solid–liquid metal interface in metal matrix composites. Metall. Mater. Trans. A **19**, 2847-2855 (1988).

[8] U. Hecht, S. Rex, On the transition from pushing to engulfment during directional solidification of the particle-reinforced aluminum-based metal-matrix composite. Metall. Mater. Trans. A **28**, 867-874 (1997).

[9] D.M. Stefanescu, F. Rana, Solidification processing of metal matrix composites. In: Metallurgical Development and Control in Materials Processing, TMS (1989), 95-100.

[10] S. Sen, B.K. Dhindaw, D.M. Stefanescu, A. Catalina, P.A. Curreri, Melt convection effects on the critical velocity of particle engulfment. J. Cryst. Growth **173**, 574-584 (1997).

[11] D.M. Stefanescu, R.V. Phalnikar, H. Pang, S. Ahuja, B.K. Dhindaw, A coupled model for the critical velocity of particle engulfment. ISIJ Int. **35**, 700-707 (1995).

[12] A.V. Catalina, S. Mukherjee, D.M. Stefanescu, A dynamic model for the interaction between a solid particle and an advancing solid/liquid interface. Metall. Mater. Trans. A **31**, 2559-2568 (2000).

[13] E. Fraś, E. Olejnik, Interaction between solidification front and alien phase particles. Arch. Metall. Mater. **53**, 695-702 (2008).

[14] G. Angella, D. Ripamonti, M. Górny, S. Masaggia, F. Zanardi, The Role of Microstructure on Tensile Plastic Behavior of Ductile Iron GJS 400 Produced through Different Cooling Rates, Part I: Microstructure. Metals **9**, 1282 (2019).
DOI: https://doi.org/10.3390/met9121282

[15] E. Fraś, M. Górny, H.F. Lopez, The Transition from Gray to White Iron during Solidification, Part I – Theoretical Background. Metall. Mater. Trans. A **36A**, 3075-3082 (2005).

[16] G. Lesoult, M. Castro, J. Lacaze, Solidification of Spheroidal Graphite Cast Iron: III Microsegregation Related Effects. Acta Mater. **47**, 3779-3792 (1999).

[17] K.M. Pedersen, N.S. Tiedje, Graphite nodule count and size distribution in thin-walled ductile cast iron. Mater. Charact. **59**, 1111-1121 (2008).

[18] ISO 945-4:2016(E), Microstructure of cast irons – Part 4, ISO, Geneva (2016).

[19] J. Friess, U. Sonntag, I. Steller et al., From Individual Graphite Assignment to an Improved Digital Image Analysis of Ductile Iron. Int. J. Metalcast. **14**, 1090-1104 (2020).
DOI: https://doi.org/10.1007/s40962-020-00416-3

[20] K. Wiencek, T. Skowronek, B. Khatemi, Graphite Particle Size Distribution in Nodular Cast Iron. Metall. Foundry Eng. **31**, 167-173 (2005).

[21] C.B. Basak, A.K. Sengupta, Development of a FDM based code to determine the 3-D size distribution of homogeneously dispersed spherical second phase. Scripta Mater. **51**, 255-260 (2004).

[22] ISO 945-1:2019, Microstructure of cast irons – Part 1, ISO, Geneva (2019).

[23] M. Górny, M. Kawalec, G. Sikora, E. Olejnik, H. Lopez, Primary Structure and Graphite Nodules in Thin-Walled High-Nickel Ductile Iron Castings. Metals **8**, 649 (2018).
DOI: https://doi.org/10.3390/met8080649

[24] M. Górny, E. Tyrała, Effect of Cooling Rate on Microstructure and Mechanical Properties of Thin-Walled Ductile Iron Castings. J. Mater. Eng. Perform. **22**, 300-305 (2013).
DOI: https://doi.org/10.1007/s11665-012-0233-0

[25] W. Menk, A new high strength high ductile nodular iron. Mater. Sci. Forum **925**, 224-230 (2018).

[26] W. Menk, European Patent EP 1270747 B1 (2007).

[27] M. Bamberger, Encyclopedia of Iron, Steel, Their Alloy, Taylor & Francis (2016), 196-216.

[28] Zanardi Fonderie, https://zanardifonderie.com, accessed: 03.05.2026.

[29] M. Górny, Ł. Gondek, E. Tyrała et al., Structure Homogeneity and Thermal Stability of Austempered Ductile Iron. Metall. Mater. Trans. A **52**, 2227-2237 (2021).
DOI: https://doi.org/10.1007/s11661-021-06214-8

[30] F. Zanardi, C. Mapelli, S. Barella, Reclassification of spheroidal graphite ductile cast irons grades according to design needs. Int. J. Metalcast. **14**, 622-639 (2020).
DOI: https://doi.org/10.1007/s40962-020-00454-x

[31] R.A. Zanardi, Method for manufacturing spheroidal cast iron mechanical components. Patent WO 2008/003395 A2 (2008).

[32] EN 16124:2011, Founding – Low-alloyed ferritic spheroidal graphite cast irons for elevated temperature applications, CEN (2011).

[33] M. Górny, J. Marosz, R. Cygan et al., Ultra-thin-walled Si-Mo SG castings reinforced with titanium–molybdenum carbides. Int. J. Metalcast. (2026).
DOI: https://doi.org/10.1007/s40962-026-01934-2

[34] B. Cygan, M. Stawarz, J. Jezierski, Heat Treatment of the SiMo Iron Castings – Case Study in the Automotive Foundry. Arch. Foundry Eng. **18**, 103-109 (2018).
DOI: https://doi.org/10.24425/afe.2018.125177

[35] M. Górny, M. Kawalec, B. Gracz, M. Tupaj, Influence of Cooling Rate on Microstructure Formation of Si–Mo Ductile Iron Castings. Metals **11**, 1634 (2021).
DOI: https://doi.org/10.3390/met11101634

[36] G. Palumbo, M. Górny, A. Bitka, Influence of the Cooling Rate on Mechanical and Corrosion Properties of Ferritic Si–Mo Ductile Cast Iron. Metall. Mater. Trans. A **54**, 2362-2373 (2023).
DOI: https://doi.org/10.1007/s11661-023-07023-x

[37] ISO 2892:2007, Austenitic cast irons – Classification, ISO, Geneva (2007).

[38] M. Bork, R. Chulist, M. Górny et al., The influence of nickel content on the structure parameters and magnetic properties of austenitic ductile iron castings. Arch. Civ. Mech. Eng. **25**, 117 (2025). DOI: https://doi.org/10.1007/s43452-025-01173-y

[39] M. Bork, M. Górny, G. Palumbo et al., Microstructure, mechanical parameters, and corrosion resistance of austenitic ductile iron castings. Arch. Civ. Mech. Eng. **25**, 268 (2025).
DOI: https://doi.org/10.1007/s43452-025-01331-2

[40] Nickel Institute, Properties and applications of Ni-Resist and ductile Ni-Resist alloys. A guide to the use of nickel-containing alloys No. 11018, 2nd ed., Nickel Institute (2022).

[41] M. Bork, M. Górny, G. Angella, J. Marosz, The impact of wall thickness on the microstructure and mechanical properties of austenitic high-nickel ductile iron. Journal of Casting & Materials Engineering, Special Issue, 1-6 (2026).
DOI: https://doi.org/10.7494/jcme.2026.si.1